234Th/238U disequilibrium and particulate organic carbon export in the northern South China Sea

ARTICLE *in* JOURNAL OF OCEANOGRAPHY · JUNE 2008

Impact Factor: 1.27 · DOI: 10.1007/s10872-008-0035-z

4 AUTHORS, INCLUDING:

Weifang Chen
Xiamen University
16 PUBLICATIONS **234** CITATIONS
SEE PROFILE

Pinghe Cai
Xiamen University
27 PUBLICATIONS **517** CITATIONS
SEE PROFILE

Minhan Dai
Xiamen University
165 PUBLICATIONS **4,012** CITATIONS
SEE PROFILE

Journal of Oceanography, Vol. 64, pp. 417 to 428, 2008

$^{234}Th/^{238}U$ Disequilibrium and Particulate Organic Carbon Export in the Northern South China Sea

Weifang Chen[1], Pinghe Cai[1], Minhan Dai[1]* and Junfeng Wei[2]

[1]*State Key Laboratory of Marine Environmental Science, Xiamen University, Xiamen 361005, China*
[2]*College of Environment and Chemical Engineering, Dalian University, Dalian 116622, China*

(Received 8 April 2007; in revised form 27 November 2007; accepted 28 November 2007)

We utilized ^{234}Th, a naturally occurring radionuclide, to quantify the particulate organic carbon (POC) export rates in the northern South China Sea (SCS) based on data collected in July 2000 (summer), May 2001 (spring) and November 2002 (autumn). Th-234 deficit was enhanced with depth in the euphotic zone, reaching a subsurface maximum at the Chl-a maximum in most cases, as commonly observed in many oceanic regimes. Th-234 was in general in equilibrium with ^{238}U at a depth of ~100 m, the bottom of the euphotic zone. In this study the ^{234}Th deficit appeared to be less significant in November than in July and May. A surface excess of ^{234}Th relative to ^{238}U was found in the summer over the shelf of the northern SCS, most likely due to the accumulation of suspended particles entrapped by a salinity front. Comparison of the ^{234}Th fluxes from the upper 10 m water column between 2-D and traditional 1-D models revealed agreement within the errors of estimation, suggesting the applicability of the 1-D model to this particular shelf region. 1-D model-based ^{234}Th fluxes were converted to POC export rates using the ratios of bottle POC to ^{234}Th. The values ranged from 5.3 to 26.6 mmol C $m^{-2}d^{-1}$ and were slightly higher than those in the southern SCS and other oligotrophic areas. POC export overall showed larger values in spring and summer than in autumn, the seasonality of which was, however, not significant. The highest POC export rate (26.6 mmol C $m^{-2}d^{-1}$) appeared at the shelf break in spring (May), when Chl-a increased and the community structure changed from pico-phytoplankton (<2 μm) dominated to nano-phytoplankton (2–20 μm) and micro-phytoplankton (20–200 μm) dominated.

Keywords:
· $^{234}Th/^{238}U$ disequilibrium,
· POC export,
· South China Sea.

1. Introduction

Recent studies have revealed the significance of continental margins in global carbon cycling (Tsunogai *et al*., 1999; Liu *et al*., 2000; Frankignoulle and Borges, 2001). Despite their relatively limited surface area, continental margins contribute ~28% of global ocean primary production (Eppley and Peterson, 1979). This forms a fundamental basis for continental margins to be potential carbon sinks, although the global pattern and magnitude still need to be better constrained (Cai and Dai, 2004; Borges *et al*., 2005; Cai *et al*., 2006).

Among many other phenomena, the export of particulate organic carbon (POC) implies the net sequestration of CO_2 and the recycling of organic matter within upper marginal seas, which represents an essential variable that ultimately determines whether a marginal system is a source or sink with respect to atmospheric CO_2. The scenario is compounded by the dynamics of a continental margin, where the typical new production concept built on the basis of steady states derived from open ocean studies is not always valid.

The disequilibrium between ^{234}Th and ^{238}U in the upper ocean has been widely utilized to quantify the particle scavenging and organic carbon export rates in open waters (see Waples *et al*., 2006). Its half-life of 24.1 days and particle-reactive nature make ^{234}Th an ideal tracer for particle export in the surface ocean on time scales of days to weeks. However, it must be pointed out that ^{234}Th measurements in coastal settings remain very limited (Wei and Murray, 1992; Cochran *et al*., 1995; Gustafsson *et al*., 1998; Benitez-Nelson *et al*., 2000; Charette *et al*., 2001). Such data-paucity hampers our ability to fully assess the role of marginal systems in the ocean carbon cycle.

* Corresponding author. E-mail: mdai@xmu.edu.cn

The South China Sea (SCS) is the second largest marginal sea in the world. It has an area of 3.5×10^6 km^2 and an average depth of ~1350 m. Evidence has emerged that the SCS is a source of atmospheric CO_2, which is substantially different from mid or high latitude marginal systems, which uptake significant amounts of CO_2 (Cai and Dai, 2004; Zhai *et al*., 2005). Studies on primary production have shown that the annual mean primary production in the SCS is ~29 mmol C m^{-2}d^{-1} based on SeaWiFS data (Liu *et al*., 2002) or 32 (summer)–45 (winter) mmol C m^{-2}d^{-1} based on field measurements (Ning *et al*., 2004). However, research on POC export and/or new production remains very limited. Cai *et al*. (2002) determined new production of 4.4–5.7 mmol C m^{-2}d^{-1} in the southern SCS. Sediment trap-derived POC export at 100 m in the northern basin of the SCS is ~2.5 mmol C m^{-2}d^{-1} (Chen *et al*., 1999). Th-234 derived POC export varies from 4.0–25.0 mmol C m^{-2}d^{-1} in autumn in the northern basin of the SCS (Chen *et al*., 1997) to 13.1–46.5 mmol C m^{-2}d^{-1} in spring in the southern SCS (Cai *et al*., 2001). It should be noted that these studies were typically based on a single cruise with very limited spatial coverage.

In this study we utilized ^{234}Th/^{238}U disequilibrium as a tracer of POC export, based on the data collected from three cruises (July 2000, May 2001 and November 2002) covering a region from shelf to slope in the northern SCS. Compared to prior research in the region, our present study had a better spatial and temporal coverage and hence may provide new insights into POC fluxes and their control in a large marginal system.

2. Methods

2.1 Study area

The northern SCS consists of the shelf, slope and deep basin regions. The Pearl River brings a large quantity of fresh water and nutrients into the shelf region. The effective water exchange between the northern SCS and the Western Pacific Ocean occurs in the Luzon Strait. Through this Strait, the Kuroshio intrudes from the Western Philippine Sea into the northern SCS and sometimes it reaches the slope in its upper 300 m (Shaw and Chao, 1994). The East Asian Monsoon prevails in the SCS, which results in a surface cyclonic circulation from November to February but an anti-cyclonic circulation from June to August (Hu *et al*., 2000).

The SCS is warm, permanently stratified and oligotrophic. The inorganic nitrogen and phosphorus concentrations in the euphotic layer are typically at the nM level (Liang *et al*., 2006). Strong vertical mixing is typical in winter, which enhances the nutrient supplies from the subsurface (Chao *et al*., 1996). Accordingly, the maximum Chl-a and primary production appear in winter (Liu

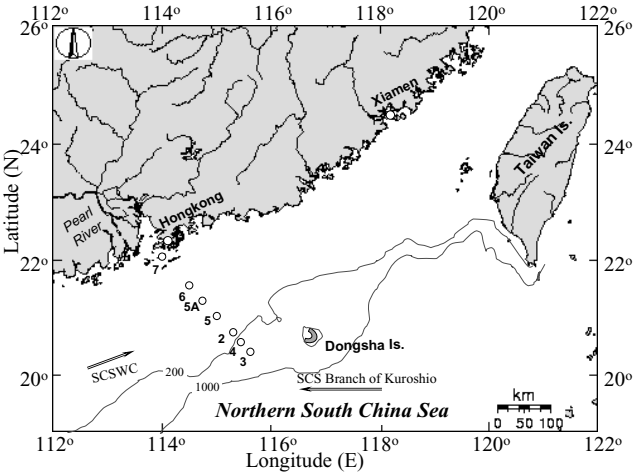

Fig. 1. Location of sampling stations in the northern South China Sea (SCS) from 2000 to 2002.

et al., 2002; Chen, 2005). The concentration of Chl-a in the surface water changes from 0.29 μg L^{-1} in winter to a low of 0.11 μg L^{-1} in summer according to Ning *et al*. (2004). Pico-phytoplankton (<2 μm in size) was reported to be dominant, contributing up to 50–75% of the total phytoplankton biomass (Ning *et al*., 2004), which is characteristic of oligotrophic regimes (Platt *et al*., 1983).

2.2 Sampling

As a part of the CAR-TTT project (CARbon Transfer, Transport and Transformation) in the Pearl River Estuary and the adjacent northern SCS, this study was carried out on three cruises on board R/V Yanping II in July–August of 2000, May–June of 2001 and November of 2002, representing summer, spring and late autumn, respectively. Sampling locations are shown in Fig. 1, and further detailed in Table 1–3.

Profiles of temperature and salinity were obtained using a SBE-19-plus CTD unit (Sea-Bird Co.). The calibration and data processing of the CTD followed the previously described procedure (Cai *et al*., 2004). All samples were collected using a CTD rosette equipped with Go-Flo bottles (General Oceanics Co.). A 20-liter portion was used for ^{234}Th analysis. Ancillary measurements involved primary productivity, nutrients, pigment and POC.

2.3 Analyses

2.3.1 POC, Chl-a

For POC analysis, four liters of seawater was filtered through a pre-combusted 47 mm GF/F filter (Whatman). POC was determined with a PE-2400 SERIES II CHNS/O analyzer according to the JGOFS protocols (Knap *et al*., 1996). Based on replicate analyses, the precision of

the POC determination was <10%.

Chl-a samples were filtered through GF/F filters (Whatman, 47 mm) immediately after sampling and determined with a spectrofluorometric method (Parsons *et al*., 1984) using a Hitach 850 fluorometer. Additional samples were filtered sequentially through a series of membrane filters with different pore sizes to obtain size-fractionated Chl-a, i.e., pico-phytoplankton (<2 μm), nano-phytoplankton (2–20 μm) and micro-phytoplankton (20–200 μm) (Wang *et al*., 1997).

2.3.2 ^{234}Th analysis

For ^{234}Th analysis, a 20-liter portion of seawater was filtered through a 142 mm diameter, 0.4 μm pore size polycarbonate membrane filter immediately after sample collection. Filters were folded and stored for the subsequent determination of particulate ^{234}Th based on the procedure described by Anderson and Fleer (1982). Concentrated HCl (50 mL) together with ~10 dpm of ^{230}Th was as a yield monitor and 100 mg of Fe^{3+} carrier were added to the filtrates. Subsequent analysis involved the co-precipitation of ^{234}Th with $Fe(OH)_3$ and the separation of ^{234}Th from its parent nuclide ^{238}U via ion-exchange chromatography onboard ship (Anderson and Fleer, 1982). Finally, ^{234}Th was extracted into a 0.25 M TTA/benzene solution, which was then evaporated on stainless steel discs. The discs were counted on a low background (~0.7 cpm) anticoincidence β-counter (Model BH 1216), which detects the β-emitting ^{234}Th daughter ^{234m}Pa. In order to obtain chemical yields of thorium, ^{230}Th was counted by alpha spectrometry on silicon surface barrier detectors (Octête^{TM} PC). The results showed that chemical recoveries of ^{234}Th generally fell in the range of 60–90%.

Several surface water samples collected during our cruises were used as ^{234}Th standards. The water samples were filtered through a 0.45 μm pore size membrane immediately after collection. The filtrates were acidified and stored for at least 4 months to ensure secular equilibrium between ^{234}Th and ^{238}U. The derived ^{234}Th activities were identical within an error of ±5% to those derived from salinity using the relationship of ^{238}U (dpm L^{-1}) = 0.07081 × S (Ku *et al*., 1977). The activities of ^{234}Th reported in this paper were all decay-corrected to the midpoint of the time of collection.

2.4 Flux estimation

In order to determine the flux of ^{234}Th from the upper ocean, and hence the extent of POC export, the following ^{234}Th activity balance equation was used:

$$\partial A_{Th}/\partial t = A_U \cdot \lambda_{Th} - A_{Th} \cdot \lambda_{Th} - P_{Th} + V, \qquad (1)$$

where $\partial A_{Th}/\partial t$ is the change in ^{234}Th activity with time; A_U is the ^{238}U activity; A_{Th} is the total ^{234}Th activity; λ_{Th} is the ^{234}Th decay constant (0.0288 d^{-1}); P_{Th} is vertical particulate flux of ^{234}Th; and V is the sum of advective and diffusive terms. In the open ocean, the steady state (SS) is often assumed (i.e., $\partial A_{Th}/\partial t = 0$) and physical processes are assumed to be negligible (i.e., $V = 0$). The magnitude of the export flux is thus mainly driven by the extent of the ^{234}Th/^{238}U disequilibrium. In most cases, the SS assumption has proven to be valid, except for periods of rapid particle export, such as during phytoplankton blooms, when significant ^{234}Th removal occurs (Buesseler *et al*., 1998). Vertical advection, which is included in the term for physical processes, V in Eq. (1), has been shown to be important in areas of intense upwelling, such as in the equatorial Pacific and along the coast of the Arabian Sea during the SW monsoon (Buesseler, 1998). Horizontal transport may be critical in coastal regions, where large horizontal gradients in ^{234}Th scavenging can occur (Gustafsson *et al*., 1998; Benitez-Nelson *et al*., 2000).

3. Results and Discussion

Surface distribution and depth profiles of ^{234}Th and other relevant parameters for the three cruises in the northern SCS are presented in Tables 1–3 and Figs. 2–3. In Fig. 3, surface ^{234}Th activities as well as salinity, POC and Chl-a are plotted against the stations, which are arranged in sequence by longitude.

3.1 Hydrological and hydrochemical settings

The northern SCS is characterized by high sea surface temperature (SST, >26°C) throughout the year. The SST ranges between 28.8–29.0°C in summer, higher than in the autumn or spring (26.2–27.9°C).

As shown in Fig. 2, the mixed layer in the northern SCS was shallow in spring and summer, generally less than 40 m, while in autumn it deepened to 100 m at Sta. 3. Surface Chl-a ranged from 0.04 μg L^{-1} to 0.18 μg L^{-1}, while the nutrients (NO_3^-, PO_4^{3-}) were below detection limits.

Further shown in Fig. 2 is the Chl-a size distribution. It is remarkable that the smallest size fraction (pico-phytoplankton) was most abundant, representing up to 70–90% of the total biomass at the offshore stations (e.g., Sta. 2 and Sta. 3), with the exception of the first visit to Sta. 2 in May 2001. This is in agreement with prior research (Ning *et al*., 2004).

The concentration of POC mostly varied between 2 and 9 μM in the top 100 m and decreased to below 2 μM at depth. A subsurface Chl-a maximum appeared immediately below the mixed layer and the peak of POC appeared around the pigment maximum at most stations (Fig. 2).

3.2 ^{234}Th-distribution

Surface dissolved ^{234}Th activities ranged from 0.49 to 2.54 dpm L^{-1}. Particulate ^{234}Th (>0.45 μm) activities

Table 1. ^{234}Th activities in the northern South China Sea during July 2000.

Station	Location	Depth	^{234}Thd	± error	^{234}Thp	± error	^{234}ThT	± error	^{238}U	POC/^{234}Th
		m	dpm L^{-1}							μmol dpm^{-1}
7	113°58′ E, 22°12′ N	1	0.487	0.074	0.470	0.054	0.957	0.092	1.50	80.4 ± 9.9
6	114°30′ E, 21°30′ N	1	2.538	0.11	0.415	0.053	2.954	0.122	2.38	28.4 ± 3.6
5	115°00′ E, 21°00′ N	1	2.363	0.13	0.189	0.053	2.552	0.140	2.37	13.0 ± 3.6
2	115°17′ E, 20°43′ N	1	1.934	0.053	0.130	0.028	2.065	0.060	2.37	15.3 ± 3.3
		10	2.204	0.21	0.182	0.026	2.386	0.212	2.38	11.8 ± 1.7
		36	1.771	0.066	0.245	0.021	2.016	0.069	2.40	17.0 ± 1.4
		63	1.626	0.055	0.265	0.034	1.890	0.065	2.42	16.4 ± 2.1
		75	1.748	0.055	0.262	0.077	2.010	0.095	2.43	11.9 ± 3.5
		150	1.927	0.064	0.294	0.035	2.221	0.073	2.45	9.0 ± 1.1
4	115°28′ E, 20°32′ N	1	2.293	0.11	0.257	0.053	2.550	0.122	2.36	23.3 ± 4.7
3a	115°38′ E, 20°21′ N	1	1.845	0.054	0.308	0.031	2.153	0.062	2.36	13.5 ± 1.4
	21/07/00	10	1.891	0.068	0.362	0.031	2.252	0.075	2.36	9.1 ± 0.8
		30	1.837	0.075	0.233	0.023	2.070	0.078	2.40	17.9 ± 1.8
		50	1.333	0.078	0.327	0.029	1.661	0.083	2.43	16.0 ± 1.4
		75	1.278	0.20	0.353	0.039	1.632	0.204	2.45	7.9 ± 0.9
		145	1.961	0.069	0.304	0.024	2.265	0.073	2.45	4.5 ± 0.4
		250	1.582	0.067	0.673	0.04	2.255	0.078	2.44	1.9 ± 0.1
3b	115°38′ E, 20°21′ N	1	1.419	0.056	0.409	0.025	1.828	0.061	2.37	7.1 ± 0.4
	27/07/00	10	1.261	0.089	0.529	0.036	1.790	0.096	2.37	5.7 ± 0.4
		30	1.282	0.056	0.150	0.021	1.432	0.060	2.39	17.5 ± 2.5
		50	1.125	0.052	0.423	0.029	1.549	0.060	2.41	8.2 ± 0.6
		75	1.382	0.061	0.452	0.026	1.834	0.066	2.43	5.3 ± 0.3
		145	1.676	0.058	0.216	0.024	1.893	0.063	2.45	6.8 ± 0.8
		250	1.958	0.067	0.330	0.039	2.288	0.078	2.44	15.4 ± 1.8

fell in the range 0.07–0.44 dpm L^{-1}, representing ~2–52% of the total activity (Tables 1–3). ^{234}Th was in general deficit relative to ^{238}U in the surface water and enhanced removal of ^{234}Th (i.e., ^{234}Th minimum) occurred at the subsurface Chl-a maxima. At the bottom of the euphotic zone (~100 m), the extent of ^{234}Th/^{238}U disequilibrium was less than or approached secular equilibrium. This stratified structure of ^{234}Th has also been observed in the southern SCS (Chen *et al*., 1997) and other oceanic regimes (Coale and Bruland, 1987), which suggests that the removal of ^{234}Th was caused mainly by fresh particles. At Sta. 5 in Nov. 2002 below 45 m, where secular equilibrium was reached, the deficit of ^{234}Th appeared once more and increased with depth. Note that Sta. 5 is located on the shelf (depth = 104 m) and sediment resuspension or cross-shelf transport is possible, which may result in a disequilibrium at depth. This is a common phenomenon in the marginal sea (Cochran *et al*., 1995; Charette *et al*., 2001).

In 2000, we had a good sampling coverage, which allowed us to examine the horizontal distribution of ^{234}Th. Following the gradient of salinity and POC, surface total ^{234}Th increased overall from the inner shelf to offshore, approaching the activity of ^{238}U at Sta. 5~Sta. 3. An exception to this occurred however at Sta. 6, where surface total ^{234}Th was in excess with respect to ^{238}U, even if analytical errors are taken into account (Fig. 3(a)). ^{234}Th excess below the euphotic zone has been observed by numerous researchers, likely due to particle remineralization or accumulation (Buesseler *et al*., 2004; Savoye *et al*., 2004). To our knowledge, except for the large ^{234}Th excess in surface water near the retreating ice edge and under the ice (Rutgers van der Loeff *et al*., 2002), such surface ^{234}Th excess has seldom been identified in low latitude areas.

A parallel study of physical settings revealed that both temperature and salinity fronts appeared to exist around Sta. 6, where the temperature and salinity gradients reached >0.054°C·km^{-1} and >0.018·km^{-1}, respectively (Zhuang *et al*., 2003). In addition, our observed high POC and particulate ^{234}Th in the surface water of Sta. 7 and Sta. 6 (Table 1; Fig. 3(c)) may also suggest an

Table 2. ^{234}Th activities in the northern South China Sea during May 2001.

Station	Location	Depth	^{234}Thd	± error	^{234}Thp	± error	^{234}ThT	± error	^{238}U	POC/^{234}Th
		m	dpm L^{-1}							μmol dpm^{-1}
2a	115.27°E, 20.72°N	1	1.689	0.082	0.101	0.008	1.790	0.082	2.39	35.9 ± 2.7
	25/05/01	10	1.290	0.040	0.077	0.007	1.367	0.040	2.40	—
		37	1.144	0.033	0.148	0.009	1.292	0.034	2.41	18.4 ± 1.1
		75	1.328	0.040	0.318	0.012	1.645	0.042	2.43	6.7 ± 0.2
		100	1.163	0.041	0.304	0.015	1.467	0.044	2.43	9.7 ± 0.5
		150	1.404	0.037	0.326	0.012	1.730	0.039	2.45	6.3 ± 0.2
		180	1.425	0.042	0.569	0.022	1.994	0.048	2.45	—
2b	115.27°E, 20.72°N	1	—	—	—	—	2.0	—	2.40	—
	29/05/01	10	1.889	0.096	0.178	0.012	2.067	0.097	2.40	18.0 ± 1.2
		37	1.931	0.083	0.114	0.010	2.045	0.084	2.41	17.3 ± 1.5
		50	1.474	0.068	0.231	0.011	1.705	0.069	2.43	13.4 ± 0.6
		75	2.089	0.092	0.266	0.010	2.356	0.093	2.45	10.5 ± 0.4
		100	1.054	0.045	0.550	0.014	1.604	0.047	2.46	9.1 ± 0.2

Table 3. ^{234}Th activities in the northern South China Sea during November 2002.

Station	Location	Depth	^{234}Thd	± error	^{234}Thp	± error	^{234}ThT	± error	^{238}U	POC/^{234}Th
		m	dpm L^{-1}							μmol dpm^{-1}
5	114.99°E, 21.00°N	1	1.888	0.046	0.182	0.008	2.070	0.046	2.40	24.1 ± 1.1
		15	2.023	0.053	0.157	0.007	2.179	0.054	2.39	11.3 ± 0.5
		30	1.984	0.054	0.126	0.024	2.110	0.059	2.39	29.3 ± 5.5
		45	2.657	0.078	0.069	0.030	2.726	0.084	2.39	—
		60	1.505	0.038	0.150	0.012	1.655	0.039	2.39	24.2 ± 1.9
		80	0.631	0.018	0.235	0.011	0.866	0.021	2.41	11.2 ± 0.5
3	115.62°E, 20.35°N	1	1.591	0.036	0.669	0.019	2.260	0.040	2.40	13.4 ± 0.4
		50	2.033	0.047	0.178	0.010	2.212	0.048	2.40	16.1 ± 0.9
		100	2.149	0.050	0.155	0.011	2.304	0.052	2.40	12.0 ± 0.8
		120	2.299	0.056	0.159	0.006	2.458	0.056	2.45	—
		150	2.307	0.057	0.158	0.006	2.465	0.058	2.44	8.4 ± 0.3
		200	2.077	0.053	0.545	0.015	2.622	0.055	2.45	2.7 ± 0.1

accumulation of particulate matter, most likely from the input of terrestrial materials and/or from stimulated phytoplankton growth. However, a high gradient of POC (–0.092 μM km^{-1}) and a negligible gradient of Chl-a (–0.0002 mg L^{-1}km^{-1}) between Sta. 6 and Sta. 5 demonstrated that stimulated phytoplankton growth was not evident. We thus contend that the observed surface excess in ^{234}Th at Sta. 6 may be related to the fronts, whereby suspended particles coherent with ^{234}Th were entrapped. Transformation of dissolved and particulate material is common in a river plume system (Dagg *et al.*, 2004), and the surface ^{234}Th excess we observed can thus be interpreted as the accumulation of particulate matter and subsequent transformation around the front.

3.3 Estimation of ^{234}Th fluxes and its uncertainty

In order to examine the influence of physical processes on the estimation of ^{234}Th fluxes, we followed the method described by Benitez-Nelson *et al.* (2000). We reduced Eq. (1) to several mathematical terms, where $\lambda(A_U - A_{Th})$ is defined as the SS term, $\partial A_{Th}/\partial t$ is defined as the non-steady state (NSS) term, and V is the term for

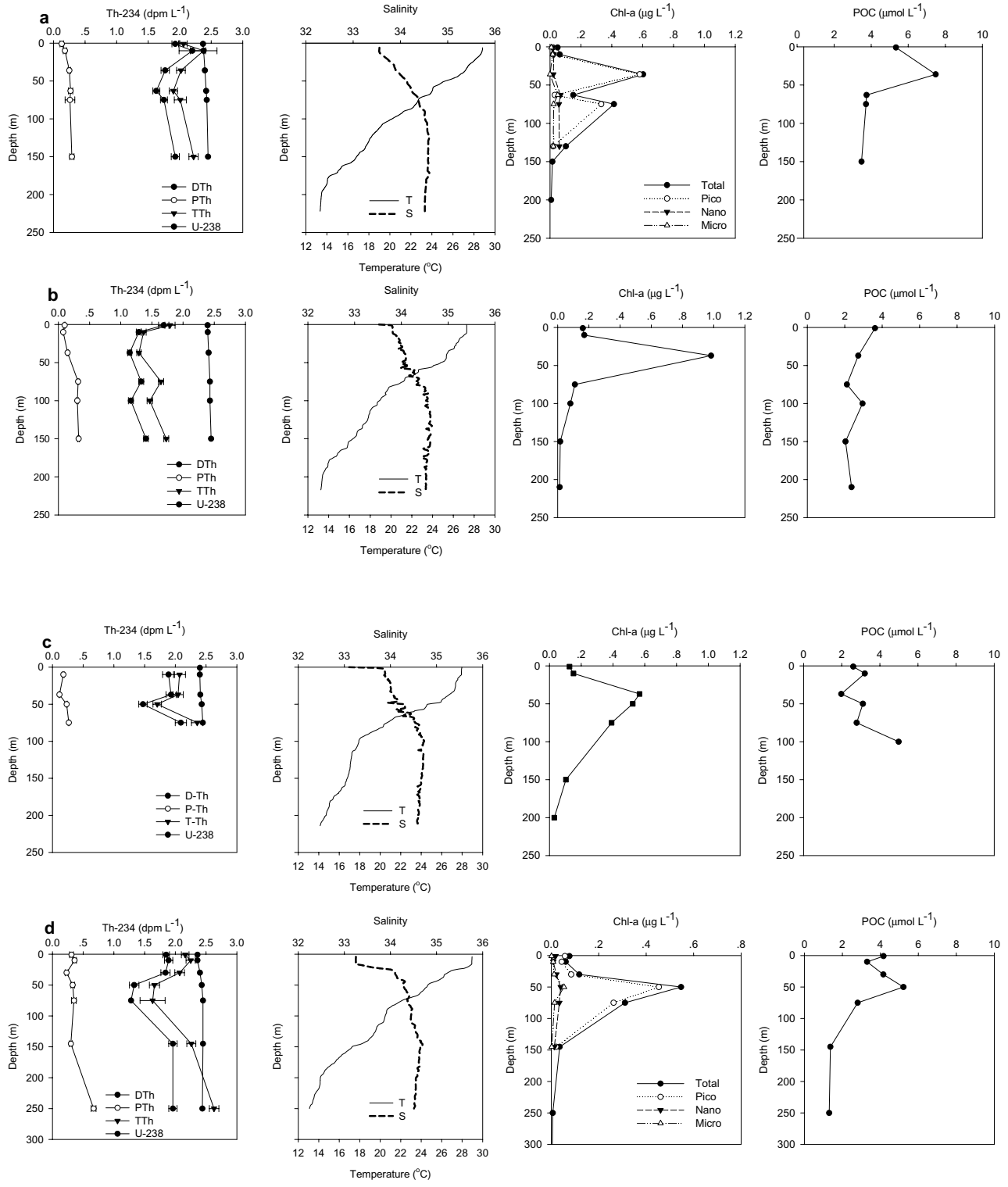

Fig. 2. Depth profiles of ^{234}Th activities, temperature and salinity, Chl-a, POC in the northern South China Sea (a: Sta. 2 on July 23, 2000; b: Sta. 2 on May 25, 2001; c: Sta. 2 on May 29, 2001; d: Sta. 3 on July 21, 2000; e: Sta. 3 on July 27, 2000; f: Sta. 3 on Nov. 13, 2002; g: Sta. 5 on Nov. 12, 2002; DTh: dissolved ^{234}Th; PTh: particulate ^{234}Th; TTh: total ^{234}Th; Pico: <2 μm; Nano: 2–20 μm; Micro: 20–200 μm).

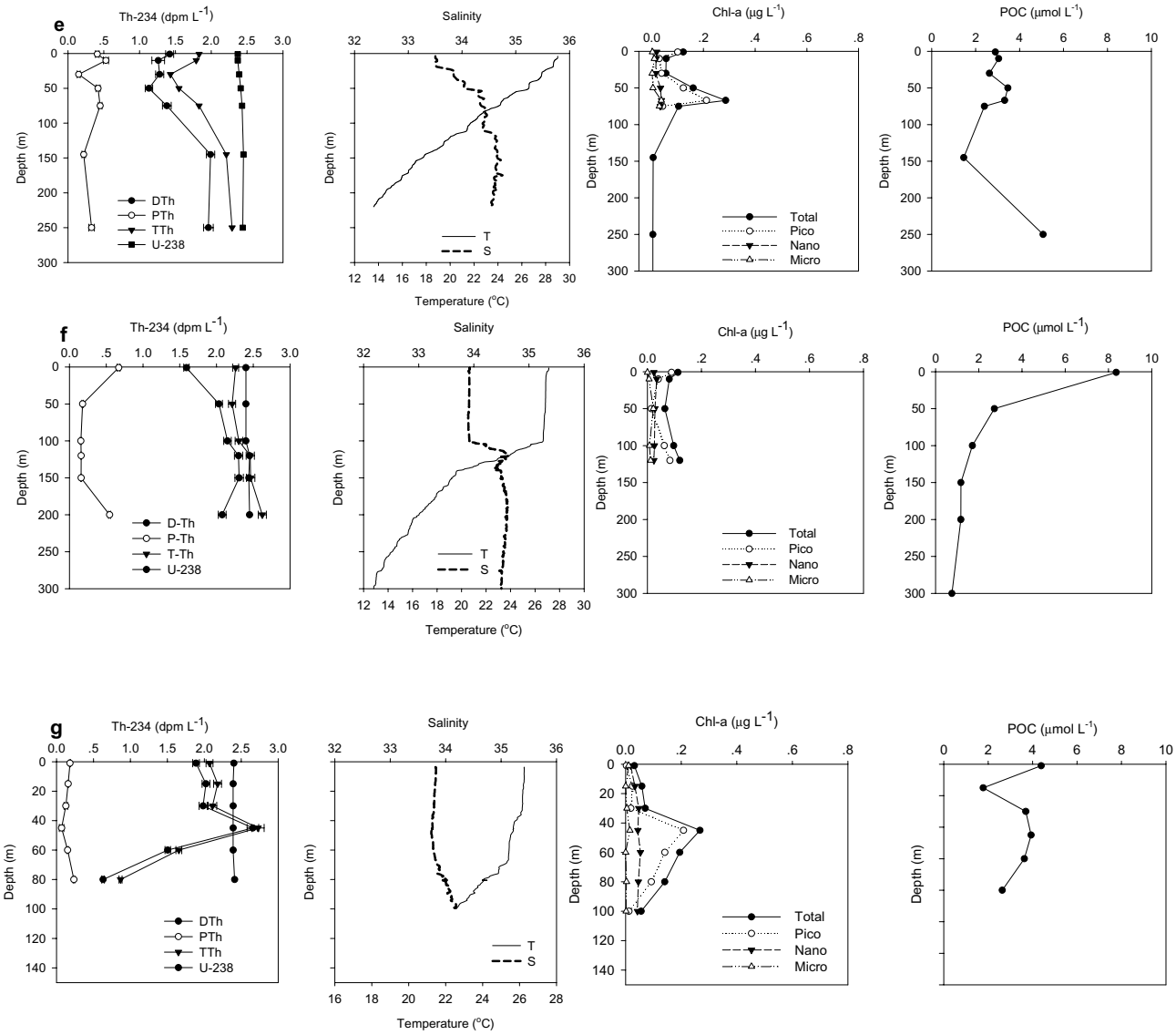

Fig. 2. (continued).

physical processes, which can be expressed as:

$$V = -u\cdot\partial A_{Th}/\partial x - v\cdot\partial A_{Th}/\partial y + K_x\cdot\partial^2 A_{Th}/\partial x^2 + K_y\cdot\partial^2 A_{Th}/\partial y^2, \quad (2)$$

where u and v are the velocity in the chosen x and y direction; $\partial A_{Th}/\partial x$, $\partial A_{Th}/\partial y$ are the activity gradient along x- and y-axis, respectively; $\partial^2 A_{Th}/\partial x^2$, $\partial^2 A_{Th}/\partial y^2$ are the second derivative of the activity distribution. In this study, alongshore transport of ^{234}Th was assumed to be negligible, i.e., $-v\cdot\partial A_{Th}/\partial y + K_y\cdot\partial^2 A_{Th}/\partial y^2 = 0$, given the scarcity of data, and this was proved to be acceptable by a previous study (Benitez-Nelson *et al*., 2000) and the observations from our current study. In order to solve Eq. (1) for P_{Th}, two additional assumptions must be invoked. First, vertical mixing (i.e., upwelling) in this region is assumed to be negligible compared to the horizontal processes and to the downward flux of particulate ^{234}Th. The vertical structure of the hydrology revealed no indication of upwelling during our survey (Fig. 3), which lent us confidence in the validity of the above assumption. Second, an SS assumption must be made for the stations without time-series occupation. This assumption has proved valid except for the period of phytoplankton bloom events (Buesseler *et al*., 1998).

With these assumptions, Eq. (1) takes the form

$$P_{Th} = A_U\cdot\lambda_{Th} - A_{Th}\cdot\lambda_{Th} + K_x\cdot\partial^2 A_{Th}/\partial x^2 - u\cdot\partial A_{Th}/\partial x, \quad (3)$$

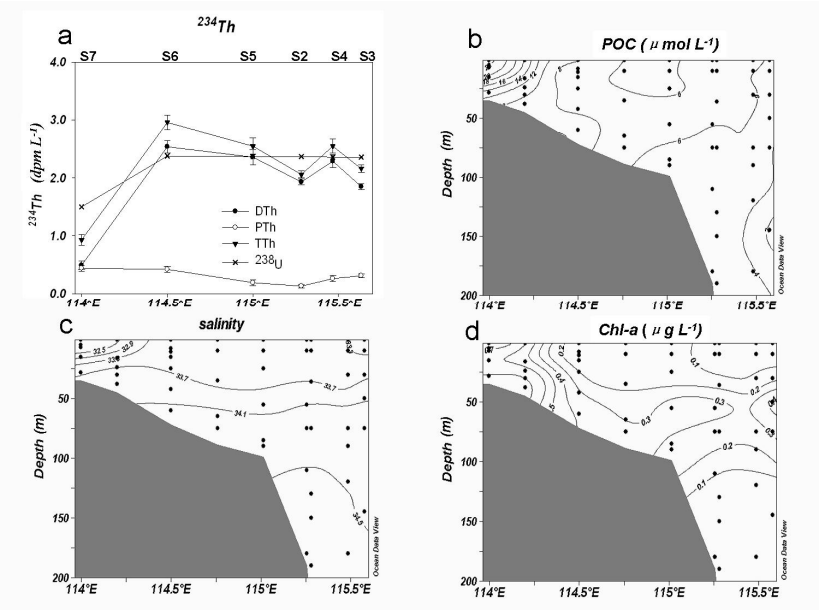

Fig. 3. Offshore distributions of (a) surface ^{234}Th activities, (b) POC, (c) salinity and (d) Chl-a in the northern South China Sea during July 2000.

Horizontal diffusivity can be estimated using empirically derived oceanic diffusivity diagrams (Okubo, 1971):

$$\log(K_x) = 1.0\log(l^{1.1}) - 1.7, \qquad (4)$$

where l is a scale of diffusion. The distance between each depth profile station ranged from 27 to 43 km during the survey, which is similar to that reported by Okubo (1971). This yields an apparent diffusivity of 2.4×10^5–7.4×10^5 cm^{2}s^{-1}, comparable with the results obtained in the Gulf of Maine (0.8×10^5–4.0×10^5 cm^{2}s^{-1}) (Benitez-Nelson *et al*., 2000).

In this study, the offshore current velocity at a specific depth was calculated using the depth profiles of zonal velocity and meridional velocity obtained by Fang *et al*. (2000). The results show that the mean offshore current velocity was ~0 cm s^{-1} at 10 m. With these estimates we calculated the ^{234}Th fluxes in the upper 10 m based on a 2-D model (Fig. 4). For comparison, the fluxes based on a traditional 1-D model were also calculated (Fig. 4). From Fig. 4, we found that, in this study, the 2-D model fluxes agreed within uncertainties with those based on the traditional 1-D model, which indicates the applicability of the 1-D model in this region. It should be pointed out that the 2-D model results are highly sensitive to diffusivity and the current velocity. For example, in this study, if we assume a typical uncertainty of ±2 cm s^{-1} for the current velocity in the upper 10 m, the calculated ^{234}Th fluxes could vary by as much as 180%. However, when ^{234}Th flux was depth-integrated to the base of the euphotic zone,

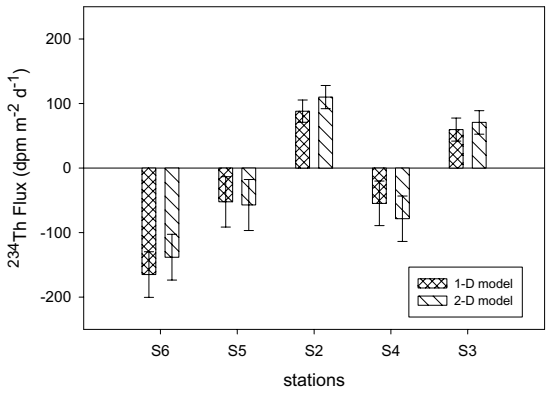

Fig. 4. ^{234}Th model flux results for the northern SCS in the upper 10 m during July 2000.

the significance of the SS term would increase. So the uncertainty from the variation of the current velocity would be reduced accordingly and it was found to be less than 10% for most of the stations in the northern SCS with the help of high resolution sampling (Chen *et al*., unpublished data). Similar scenarios were also found elsewhere in the southern SCS (Cai *et al*., 2007) and the Gulf of Maine (Charette *et al*., 2001).

In this context, we applied the 1-D model and P_{Th} was depth-integrated to the base of the euphotic zone. The ^{234}Th fluxes ranged from 441 ± 68 to 2739 ± 44 dpm m^{-2}d^{-1} in the northern SCS (Table 4), comparable to

Table 4. ^{234}Th and POC fluxes in the northern South China Sea from 2000 to 2002.

Station	Depth	PTh, dpm m^{-2}d^{-1}		POC/Th, μmol dpm^{-1}		PPOC, mmol m^{-2}d^{-1}	
	m	value	± error	value	± error	value	± error
Jul. 2000							
2	10	45	32	11.8	1.7	0.5	0.4
	36	187	89	17.0	1.4	3.2	1.5
	63	537	96	16.4	2.1	8.8	1.9
	75	699	98	11.9	3.5	8.3	2.7
3a	10	40	13	9.1	0.8	0.4	0.1
	30	167	34	17.9	1.8	3.0	0.7
	50	484	47	16.0	1.4	7.7	1.0
	75	1056	92	7.9	0.9	8.3	1.2
3b	10	161	15	5.7	0.4	0.9	0.1
	30	605	36	17.5	2.5	10.6	1.6
	50	1129	43	8.2	0.6	9.3	0.8
	75	1655	54	5.3	0.3	8.8	0.6
May 2001							
2a	10	235	13	—	—	—	—
	37	1069	24	18.4	1.1	19.7	1.2
	75	2110	38	6.7	0.2	14.1	0.6
	100	2739	44	9.7	0.5	26.6	1.4
2b	10	—	—	18.0	3.2	—	—
	37	269	50	17.3	2.0	4.7	1.0
	50	472	54	13.4	3.1	6.3	1.6
	75	765	68	10.5	2.8	8.0	2.2
	100	1106	78	9.1	5.0	10.0	5.6
Nov. 2002							
5	15	117	15	11.3	0.5	1.3	0.2
	30	223	23	29.3	5.5	6.5	1.4
	45	211	32	57.4	25.2	12.1	5.6
	60	297	38	24.2	1.9	7.2	1.1
	80	953	40	11.2	0.5	10.7	0.7
3	50	236	45	16.1	0.9	3.8	0.8
	100	441	68	12.0	0.8	5.3	0.9
	120	466	71	—	—	—	—
	150	452	80	8.4	0.3	3.8	0.7

the results of Chen *et al*. (1997) in the same region (900–1300 dpm m^{-2}d^{-1}) and those of Charette *et al*. (2001) in the Gulf of Maine (1120–2960 dpm m^{-2}d^{-1}).

3.4 ^{234}Th-derived POC export in the northern SCS

To a first order of approximation, the SS 1-D model ^{234}Th fluxes were converted to POC export fluxes using the POC/^{234}Th ratios on suspended particles at the base of the euphotic zone (Table 4). We used a combination of bottle POC data (4 L filtered onto GF/F filters) and 20 L particulate ^{234}Th samples (filtered onto 0.4 μm membrane filters) for the determination of POC/^{234}Th on particles. The POC/^{234}Th ratios at the base of the euphotic zone ranged from 5 to 14 μmol dpm^{-1}. As shown in Tables 1–3, POC/^{234}Th ratios tended to decrease with depth at all stations, except for the measurements near the seafloor, where the re-suspension of sediments may provide an additional source of POC, resulting in high POC/^{234}Th ratios. The decline in POC/^{234}Th ratios with depth indicates a preferential remineralization of POC relative to

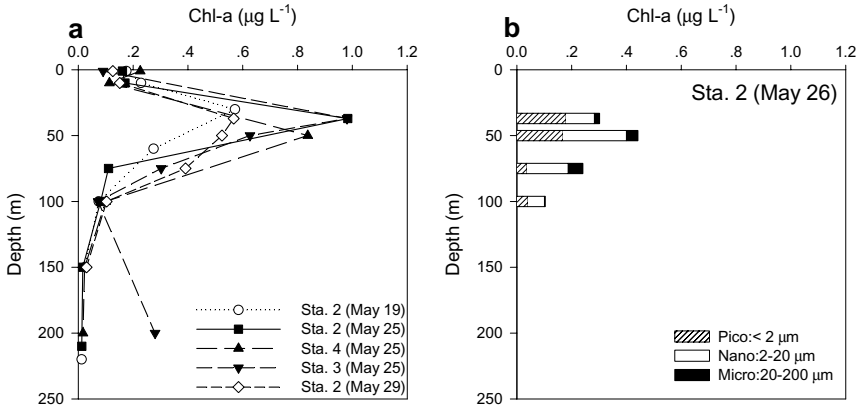

Fig. 5. (a) Depth profiles of Chl-a at the outer shelf; (b) size-fractionated Chl-a at Sta. 2 in May 2001 (Pico: <2 μm; Nano: 2–20 μm; Micro: 20–200 μm). Data are from Dai *et al.* (2007).

^{234}Th, as previously suggested (Buesseler *et al.*, 2006; Cai *et al.*, 2006b). The depth profiles of size-fractionated POC/^{234}Th ratio collected from the northern SCS during other cruises showed that bottle POC/^{234}Th ratios were consistently higher by a factor of 2–3 than those on large particles determined using an *in-situ* pump (Chen *et al.*, in preparation). Thus, using bottle POC/^{234}Th ratios allowed us to place a constraint on the upper limit of the export fluxes of POC in the study area.

Here the depth of the euphotic zone is defined as the penetration depth of 1% light and it is mostly located at ~100 m. As shown in Table 4, the POC export fluxes out of the euphotic zone ranged from 5.3 ± 0.9 to 26.6 ± 1.4 mmol C m^{-2}d^{-1}, comparable to other continental margins (Benitez-Nelson *et al.*, 2000; Charette *et al.*, 2001) but slightly elevated as compared to the southern SCS (~3.8 mmol C m^{-2}d^{-1}, Cai *et al.*, 2007). No evident inter-annual variation was found at Sta. 3 when comparing our POC export (5.3 ± 0.9 mmol C m^{-2}d^{-1} in November 2002) with that of 4.0 mmol C m^{-2}d^{-1} in September 1994 from Chen *et al.* (1997). Our seasonal pattern of ^{234}Th deficit and POC flux does not show elevated export in November as compared to that in July. This contrasts with the seasonal variation of primary production in the entire SCS (Liu *et al.*, 2002) and POC export in the northern SCS (Chen *et al.*, 1999). For example, primary production and POC export typically peak in November–February (Chen *et al.*, 1999; Liu *et al.*, 2002). The available data do not allow us to further address this issue, which requires higher spatial and temporal resolution of ^{234}Th sampling.

The maxima of ^{234}Th deficit and POC flux were found during the first visit to Sta. 2 in May 2001 (Fig. 2, Table 4). At the beginning of this cruise there was a bloom from the inner shelf to Sta. 5. Although the bloom signal disappeared at Sta. 5, where the plume diminished (Dai *et al.*, 2007), a change of the Chl-a and community structure was observed at Sta. 2 (Figs. 2 and 5). From Figs. 2 and 6 it is obvious that Chl-a at the outer shelf increased on May 25 after the heavy rain and was higher than other seasons, especially in the subsurface layer. Despite the lack of information about the community structure on May 25, the survey on May 26 demonstrated that the community structure changed from pico-phytoplankton dominated to nano-phytoplankton and micro-phytoplankton dominated (Fig. 5). Previous studies have shown that large phytoplankton contributed more efficiently to POC export because larger particles sink more rapidly (Buesseler, 1998; Savoye *et al.*, 2004; Buesseler *et al.*, 2006).

4. Summary

In this paper we have presented the POC export fluxes over the northern SCS, measured using the naturally occurring radionuclide ^{234}Th. Over the shelf, depth profiles of ^{234}Th activity were found to be well stratified, which was linked to the subsurface chlorophyll a maximum. An excess in surface ^{234}Th relative to ^{238}U was observed in the northern SCS. We suggest that this excess was probably due to the accumulation of suspended particles at the front.

To a first order approximation, the SS 1-D model ^{234}Th export and the ratio of bottle POC to ^{234}Th were used to calculate the fluxes of POC export. The derived POC export fluxes ranged from 5.3 to 26.6 mmol C m^{-2}d^{-1}, which was moderately high compared to an oligotrophic area. In this study ^{234}Th deficit and POC flux appeared less significant in November than in July. A decoupling of the seasonal pattern between primary production and POC export was observed and this needs further study. The maximum POC export was shown in the first visit to Sta. 2, probably related to the change of community structure from pico-phytoplankton dominated to nano-phytoplankton and micro-phytoplankton dominated.

We should point out that the SS assumption invoked in this study remains unvalidated.

While we contend that this study has improved our understanding of the temporal changes of POC export in this important and complex marginal sea system, we are aware that the sampling resolution both in time and space remains limited, due primarily to the fact that the technique we adopted to measure ^{234}Th in this study was the $Fe(OH)_3$ precipitation method, which is extremely labor intensive and requires large volume samples, which are usually difficult to obtain frequently during typical sampling campaigns. As previously recommended by Cai *et al*. (2006a, 2008), with technological advances, the small-volume ^{234}Th method is preferable for the determination of total ^{234}Th in seawater. It can now be used onboard a research vessel for initial ^{234}Th counting with minimal water volume, and so is feasible with CTD rosette water sampling systems. It is thus capable of mapping ^{234}Th fluxes at a higher spatial and temporal resolution. In particular, we recommend the small-volume MnO_2 precipitation technique with the addition of a yield monitor, since all losses of ^{234}Th due to colloidal complexation and physical losses of MnO_2 precipitates can be corrected for by Th recoveries (Pike *et al*., 2005; Cai *et al*., 2006a; Rodriguez y Baena *et al*., 2006).

Acknowledgements

This research was supported by the Natural Science Foundation of China through Grants #49825111, #40176025, #40228007 and #90211020. Wuqi Ruan and Fan Zhang along with the crew of Yanping II provided much help during the cruises. We appreciate the assistance of Zhaozhang Chen, Ganning Zeng and Aijia Zhu with CTD data collection and processing. We also give thanks to Bangqin Huang for providing the pigment data. We are grateful to Chen-Tung Arthur Chen, and three anonymous reviewers for their comments. John Hodgkiss is thanked for his assistance with our English.

References

Anderson, R. F. and A. P. Fleer (1982): Determination of natural actinides and plutonium in marine particulate material. *Anal. Chem*., **54**, 1142–1147.

Benitez-Nelson, C. R., K. O. Buesseler and G. Crossin (2000): Upper ocean carbon export, horizontal transport, and vertical eddy diffusivity in the southwestern Gulf of Maine. *Cont. Shelf Res*., **20**, 707–736.

Borges, A. V., B. Delille and M. Frankignoulle (2005): Budgeting sinks and sources of CO_2 in the coastal ocean: Diversity of ecosystems counts. *Geophys. Res. Lett*., **32**, doi:10.1029/2005GL023053.

Buesseler, K., L. Ball, J. Andrews, C. Benitez-Nelson, R. Belastock, F. Chai and Y. Chao (1998): Upper ocean export of particulate organic carbon in the Arabian Sea derived from thorium-234. *Deep-Sea Res. II*, **45**, 2461–2487.

Buesseler, K. O. (1998): The decoupling of production and particulate export in the surface ocean. *Global Biogeochem. Cycles*, **12**, 297–310.

Buesseler, K. O., J. E. Andrews, S. M. Pike and M. A. Charette (2004): The effects of iron fertilization on carbon sequestration in the Southern Ocean. *Science*, **304**, 414–417.

Buesseler, K. O., C. R. Benitez-Nelson, S. B. Moran, A. Burd, M. A. Charette, J. K. Cochran, L. Coppola, N. S. Fisher, S. W. Fowler, W. D. Gardner, L. D. Guo, O. Gustafsson, C. Lamborg, P. Masque, J. C. Miquel, U. Passow, P. H. Santschi, N. Savoye, G. Stewart and T. Trull (2006): An assessment of particulate organic carbon to thorium-234 ratios in the ocean and their impact on the application of ^{234}Th as a POC flux proxy. *Mar. Chem*., **100**, 213–233.

Cai, P., Y. Huang, M. Chen, G. Liu and Y. Qiu (2001): Export of particulate organic carbon estimated from ^{234}Th-^{238}U disequilibria and its temporal variation in the South China Sea. *Chinese Sci. Bull*., **46**, 1722–1726 (in Chinese).

Cai, P., Y. Huang, M. Chen, L. Guo, G. Liu and Y. Qiu (2002): New production based on ^{228}Ra-derived nutrient budgets and thorium-estimated POC export at the intercalibration station in the South China Sea. *Deep-Sea Res. I*, **49**, 53–66.

Cai, P., M. Dai, D. Lv and W. Chen (2006a): An improvement in the small-volume technique for determining thorium-234 in seawater. *Mar. Chem*., **100**, 282–288.

Cai, P., M. Dai, W. Chen, T. Tang and K. Zhou (2006b): On the importance of the decay of ^{234}Th in determining size-fractionated C/^{234}Th ratio on marine particles. *Geophys. Res. Lett*., **33**, doi:10.1029/2006GL027792.

Cai, P., W. Chen, M. Dai, Z. Wan, D. Wang, Q. Li, T. Tang and D. Lv (2007): A high-resolution study of particle export in the southern South China Sea based on ^{234}Th:^{238}U disequilibrium. *J. Geophys. Res*. (in press).

Cai, P., M. Dai, D. Lv and W. Chen (2008): Reply to comment by Chin-Chang Hung *et al*. on "How accurate are ^{234}Th measurements in seawater based on the MnO_2-impregnated cartridge technique?". *Geochem. Geophys. Geosyst*., **9**, doi:10.1029/2007GC001837.

Cai, W. and M. Dai (2004): Comment on "Enhanced open ocean storage of CO_2 from shelf sea pumping". *Science*, **306**, 1477C.

Cai, W., M. Dai, Y. Wang, W. Zhai, T. Huang, S. Chen, F. Zhang, Z. Chen and Z. Wang (2004): The biogeochemistry of inorganic carbon and nutrients in the Pearl River estuary and the adjacent Northern South China Sea. *Cont. Shelf Res*., **24**, 1301–1319.

Cai, W., M. Dai and Y. Wang (2006): Air-sea exchange of carbon dioxide in ocean margins: A province-based synthesis. *Geophys. Res. Lett*., **33**, doi:10.1029/2006GL026219.

Chao, S., P. Shaw and S. Wu (1996): Deep water ventilation in the South China Sea. *Deep-Sea Res. I*, **43**, 445–466.

Charette, M. A., S. B. Moran, S. M. Pike and J. N. Smith (2001): Investigating the carbon cycle in the Gulf of Maine using the natural tracer thorium-234. *J. Geophys. Res.-Oceans*, **106**, 11553–11579.

Chen, J., M. Wiesner, H. Wong, L. Zheng, L. Xu and S. Zheng (1999): Vertical changes of POC flux and indicators of early degradation of organic matter in the South China Sea. *Sci. in China (Ser. D)*, **42**, 120–128 (in Chinese).

Chen, M., Y. Huang, F. Chen, Y. Qiu, M. Xu and D. Jiang (1997): Particle dynamics in the euphotic zone-VI. The utility of tracer ^{234}Th for studying particle dynamics in the upper water column of the Northeastern South China Sea. *J. Tropical Oceanogr.*, **16**, 91–103 (in Chinese).

Chen, Y. L. L. (2005): Spatial and seasonal variations of nitrate-based new production and primary production in the South China Sea. *Deep-Sea Res. I*, **52**, 319–340.

Coale, K. H. and K. W. Bruland (1987): Oceanic stratified euphotic zone as elucidated by ^{234}Th:^{238}U disequilibria. *Limnol. Oceanogr.*, **32**, 189–200.

Cochran, J. K., C. Barnes, D. Achman and D. T. Hirschberg (1995): Thorium-234/Uranium-238 disequilibrium as an indicator of scavenging rates and particulate organic carbon fluxes in the Northeast Water Polynya, Greenland. *J. Geophys. Res.*, **100**, 4399–4410.

Dagg, M., R. Benner, S. Lohrenz and D. Lawrence (2004): Transformation of dissolved and particulate materials on continental shelves influenced by large rivers: plume processes. *Cont. Shelf Res.*, **24**, 833–858.

Dai, M., W. Zhai, W. Cai, J. Callahan, B. Huang, S. Shang, T. Huang, X. Li, Z. Lu, W. Chen and Z. Chen (2007): Effects of an estuarine plume-associated bloom on the carbonate system in the lower reaches of the Pearl River estuary and the coastal zone of the northern South China Sea. *Cont. Shelf Res.* (in press).

Eppley, R. W. and B. J. Peterson (1979): Particulate organic matter flux and planktonic new production in the deep ocean. *Nature*, **282**, 677–680.

Fang, W., P. Shi, Q. Mao and Z. Gan (2000): Variation of upper ocean in the northern South China Sea from mooring station observations. *Acta Oceanol. Sinica*, **22**, 23–30 (in Chinese).

Frankignoulle, M. and A. V. Borges (2001): European continental shelf as a significant sink for atmospheric carbon dioxide. *Global Biogeochem. Cycles*, **15**, 569–576.

Gustafsson, O., K. O. Buesseler, W. R. Geyer, S. B. Moran and P. M. Gschwend (1998): An assessment of the relative importance of horizontal and vertical transport of particle-reactive chemicals in the coastal ocean. *Cont. Shelf Res.*, **18**, 805–829.

Hu, J., H. Kawamura, H. Hong and Y. Qi (2000): A review on the currents in the South China Sea: Seasonal circulation, South China Sea warm current and Kuroshio intrusion. *J. Oceanogr.*, **56**, 607–624.

Knap, A., A. Michaels, A. Close, H. Ducklow and A. Dickson (1996): Protocols for the Joint Global Ocean Flux Study (JGOFS) Core Measurements. JGOFS Report Nr. 19, vi+170 pp. Reprint of the IOC Manuals and Guides No. 29, UNESCO 1994.

Ku, T. L., K. G. Knauss and G. G. Mathieu (1977): Uranium in open ocean: Concentration and isotopic composition. *Deep-Sea Res.*, **24**, 1005–1017.

Liang, Y., D. Yuan, Q. Li and Q. Lin (2006): Flow injection analysis of nanomolar level orthophosphate in seawater with solid phase enrichment and colorimetric detection. *Mar. Chem.*, **103**, 122–130.

Liu, K. K., L. Atkinson, C. T. A. Chen, S. Gao, J. Hall, R. W. Macdonald, L. Talaue McManus and R. Quiñones (2000): Exploring continental margin carbon fluxes on a global scale. *EOS, Trans., AGU*, **81**, 641–644.

Liu, K. K., S. Y. Chao, P. T. Shaw, G. C. Gong, C. C. Chen and T. Y. Tang (2002): Monsoon-forced chlorophyll distribution and primary production in the South China Sea: observations and a numerical study. *Deep-Sea Res. I*, **49**, 1387–1412.

Ning, X., F. Chai, H. Xue, Y. Cai, C. Liu and J. Shi (2004): Physical-biological oceanographic coupling influencing phytoplankton and primary production in the South China Sea. *J. Geophys. Res.*, **109**, doi:10.1029/2004JC002365.

Okubo, A. (1971): Oceanic diffusion diagrams. *Deep-Sea Res.*, **18**, 789–802.

Parsons, T., Y. Maita and C. Lalli (1984). *A Manual of Chemical and Biological Methods for Seawater Analysis*. Pergamon Press, New York, 107–109, 115–122.

Pike, S. M., K. O. Buesseler, J. A. Andrews and N. Savoye (2005): Quantification of ^{234}Th recovery in small volume sea water samples by inductively coupled plasma mass spectrometry. *J. Radioanal. Nuclear Chem.*, **263**, 355–360.

Platt, T., D. V. S. Rao and B. Irvin (1983): Photosynthesis of picoplankton in the oligotrophic ocean. *Nature*, **301**, 702–704.

Rodriguez y Baena, A. M., J. C. Miquel, P. Masqué, P. P. Povinec and J. La Rosa (2006): A single vs. double spike approach to improve the accuracy of ^{234}Th measurements in small-volume seawater samples. *Mar. Chem.*, **100**, 269–281.

Rutgers van der Loeff, M. M., K. Buesseler, U. Bathmann, I. Hense and J. Andrews (2002): Comparison of carbon and opal export rates between summer and spring bloom periods in the region of the Antarctic Polar Front, SE Atlantic. *Deep-Sea Res. II*, **49**, 3849–3869.

Savoye, N., K. O. Buesseler, D. Cardinal and F. Dehairs (2004): ^{234}Th deficit and excess in the Southern Ocean during spring 2001: particle export and mineralization. *Geophys. Res. Lett.*, **31**, doi:10.1029/2004GL019744.

Shaw, P. and S. Chao (1994): Surface circulation in the South China Sea. *Deep-Sea Res. I*, **41**, 1663–1683.

Tsunogai, S., S. Watanabe and T. Sato (1999): Is there a "continental shelf pump" for the absorption of atmospheric CO_2? *Tellus B-Chemical and Physical Meteorology*, **51**, 701–712.

Wang, H. L., B. Q. Huang and H. Hong (1997): Size-fractionated productivity and nutrient dynamics of phytoplankton in subtropical coastal environments. *Hydrobiologia*, **352**, 97–106.

Waples, J. T., C. Benitez-Nelson, N. Savoye, M. M. Rutgers van der Loeff, M. Baskaran and Ö. Gustafsson (2006): An introduction to the application and future use of ^{234}Th in aquatic systems. *Mar. Chem.*, **100**, 166–189.

Wei, C. L. and J. W. Murray (1992): Temporal variations of ^{234}Th activity in the water column of Dabob Bay: Particle scavenging. *Limnol. Oceanogr.*, **37**, 296–314.

Zhai, W. D., M. H. Dai, W. J. Cai, Y. C. Wang and H. S. Hong (2005): The partial pressure of carbon dioxide and air-sea fluxes in the northern South China Sea in spring, summer and autumn. *Mar. Chem.*, **96**, 87–97.

Zhuang, W., J. Hu, Z. He, G. Zeng and Z. Chen (2003): An analysis on surface temperature and salinity from Southern Taiwan strait to Zhujiang River Estuary during July–August, 2000. *J. Tropical Oceanogr.*, **22**, 69–76 (in Chinese).